PCCP

PAPER

View Article Online
View Journal | View Issue

Cite this: *Phys. Chem. Chem. Phys.*, 2014, **16**, 24216

Theoretical analysis of the intermolecular interactions in naphthalene diimide and pyrene complexes†

Mei-Yu Yeh and Hsin-Chieh Lin*

Received 28th August 2014,
Accepted 26th September 2014

DOI: 10.1039/c4cp03879g

www.rsc.org/pccp

Supramolecular assembly of donor–acceptor complexes as the key component in organic functional nanomaterials is a promising approach for future electronic devices. One representative example of the donor–acceptor complexes is the naphthalene diimide–pyrene (NDI–Py) system, which shows fascinating photoelectric properties. Herein, the analysis of the π–π interactions between NDI and Py has been investigated using the DFT/M06-2X and reduced density gradient methods. According to the calculations, the attractive forces for the stabilization of the NDI–Py dimer are dependent on the rotation angles, which provide physical insight into the experimental data reported by Wilson and co-workers (*Langmuir*, 2011, **27**, 6554). Our results not only provide computational evidence for the origin of the rotation in the crystal structure of the NDI–Py but also address the role of the charge-transfer attractions in the complexes.

1. Introduction

Supramolecular assembly of π-conjugated molecules is a promising approach for modulating electro-optical properties of the building block depending on the nature of assembly.[1] The control of molecular packing into well-defined nanostructures from electronically and optically active molecules is considered as an important approach to fabricate electronic nanodevices.[2] Over the last two decades, researchers have developed and accumulated enormous knowledge to generate a diverse range of supramolecular nanostructures and materials,[3] both in organic and aqueous medium, by virtue of utilizing various non-covalent forces, such as π-stacking (electrostatic and dispersion interactions), charge-transfer (CT) interactions, hydrogen bonding, and metal–ligand coordination. Charge-transfer assemblies with alternate organization of donor (D) and acceptor (A) aromatic molecules are of great importance because of their inherent conducting properties.[4,5] In addition, the design of donor–acceptor (D–A) complexes have been used to create many elegant supramolecular materials, such as supramolecular photosystems,[6] rotaxanes and catenanes,[7] synthetic ion channels,[8] liquid crystals,[9] foldamers,[10] polymers,[11] nanoparticles,[12] hydrogels,[13] and organogels.[14] More recently, mixed D–A crystals have been shown to exhibit promising ambipolar charge transport properties[15,16] and room-temperature ferroelectricity.[17] These novel functions have encouraged researchers to revisit the design of CT nanostructures, as they can be prepared by molecular self-assembly in solution and would be of great significance in organic nanosized electronics.[18,19]

Since CT complexes have received intensive attention in the recent past owing to the excellent performance in organic nanodevices, understanding when specific π-conjugated systems will generate well-defined π-stacks is of fundamental importance to the fields of supramolecular and materials chemistry.[20,21] Naphthalene diimide (NDI)-derivatives[22] have been selected as building blocks for the creation of various self-assembled CT systems because of their electron-accepting nature, propensity for π-stacking, and n-type semiconductivity.[23] Ghosh *et al.* have studied the hydrazide derivative of the NDI as an acceptor formed vesicular aggregates which could intercalate the Py donor through alternating D–A based CT interactions. The presence of Py exhibited modulation of the nanostructure from vesicles to 1-D nanofibers in the formation of the CT assembly, reiterating the role of the D–A complex in influencing the nanostructures of aggregates.[24,25] George *et al.* have shown that NDI–Py amphiphilic designs offer an efficient way to construct extended nanostructured assemblies with tunable morphology.[26] Yang *et al.* have systematically studied NDI-based D–A copolymers and understood the electron donating capability of the donor portions for applications in organic field-effect transistors (OFETs) based on NDI chromophores.[27] More importantly, Wilson *et al.* have observed, from X-ray diffraction experiments, a rotation angle of about 53° for the NDI–Py packing in the crystal.[28,29]

Department of Materials Science and Engineering, National Chiao Tung University, Hsinchu, Taiwan 300, Republic of China. E-mail: hclin45@nctu.edu.tw

† Electronic supplementary information (ESI) available: The binding energies for selected configurations of the pyrene (Py), naphthalene diimide (NDI) and NDI–Py dimers, binding energies of NDI–Py dimers in the S, SP-L and SP-S configurations as a function of rotation angles, natural bond orbital (NBO) analysis data for NDI–Py heterodimers as well as NDI and Py monomers, and a side view of visualization of the interactions in real space. See DOI: 10.1039/c4cp03879g

In this work, our focus here is to study the non-covalent interactions of the NDI–Py dimer and to investigate the origin of the rotation of the NDI–Py complexes in the crystal by the DFT/M06-2X method. Although a number of theoretical methods can be used to treat weak π–π interactions such as MP2 and CCSD(T), the more feasible option would be the density functional theory (DFT) that allows the treatment of large molecular systems with reasonable computational cost. While conventional DFT functionals such as B3LYP perform poorly for non-covalent interactions (*e.g.* π-stacking), the M06 family of functionals[30] has been proven to provide accurate geometries and energies for a variety of dispersion-dominated systems such as DNA base pair stacks and benzene aggregates.[31] We firstly studied the potential energy curves of rotation in the NDI–Py system and found that the absolute minimum is obtained for the parallel sandwich (S) configuration with the rotation angles larger than 50°, which is consistent with the X-ray experimental data of the NDI–Py cocrystal (53°) reported by Wilson *et al.*[28] In addition, we also investigated the correlation between binding energy and charge-transfer attractions in the dimer of the NDI–Py.

2. Computational methods

The geometries of the isolated monomers were first calculated at the DFT/B3LYP level with a 6-31G(d) basis set.[32,33] The optimized monomers are subsequently used for constructing the homo-and hetero-dimers. The binding energies of the dimers were calculated using the M06-2X functional with 6-31G(d), 6-31G(d,p), 6-31++G(d,p) and 6-311++G(d,p) basis sets, as implemented in the Gaussian 09 program.[34]

Binding energies of the dimers were calculated as:

$$E = E_{\text{dimer}} - (E_{\text{monomer1}} + E_{\text{monomer2}}) + \text{BSSE}$$

for homodimer, where $E_{\text{monomer1}} = E_{\text{monomer2}}$ represents the energy of NDI or Py and E_{dimer} represents the energy of the NDI–dimer or Py dimer; for the heterodimer, E_{monomer1}, E_{monomer2}, and E_{dimer} represent the energy of NDI, Py and the NDI–Py dimer respectively. The basis set superposition error (BSSE) approach was incorporated into the calculations *via* the counterpoise (CP) method proposed by Boys and Bernardi.[35] The population analysis has also been performed by the natural bond orbital method[36] at the M06-2X/6-311++G(d,p) level of theory using the natural bond orbital (NBO) program.[37] The visualization of weak interactions was conducted using Multiwfn 2.6 software[38] in real space. The wave functions were generated using the Gaussian09 program at the M06-2X/6-311++G(d,p) level. The Multiwfn 2.6 deals with reduced density gradient (RDG) in real space according to the following equation:

$$\text{RDG}(r) = \frac{1}{2 \times (3 \times \pi^2)^{\frac{1}{3}}} \times \frac{|\nabla \rho(r)|}{\rho(r)^{\frac{4}{3}}}$$

where $\rho(r)$ is the electron density and can be defined as:

$$\rho(r) = \sum_i \eta_i |\varphi_i(r)|^2 = \sum_i \eta_i \left| \sum_j C_{j,i} \chi_j(r) \right|^2$$

where φ is the orbital wave function generated by M06-2X/6-311++G(d,p) mentioned above, η_i is the occupation number of orbital i, χ is basis function. C is the coefficient matrix, the element of ith row jth column corresponds to the expansion coefficient of orbital j with respect to basis function i. The graphic displays of π–π interactions were then drawn using VMD 1.9. This visualization method was successfully and widely used in many other studies.[39,40]

3. Results and discussion

In general, a face-to-face packing of large polycyclic aromatic systems can maximize the dispersion forces between molecules.[41] Therefore, we have considered a cofacial parallel sandwich (S) configuration and two slipped parallel dimers with the shift along the long (SP-L) or the short (SP-S) axis of the monomer for Py, NDI as well as NDI–Py dimers (Fig. 1). All calculations were

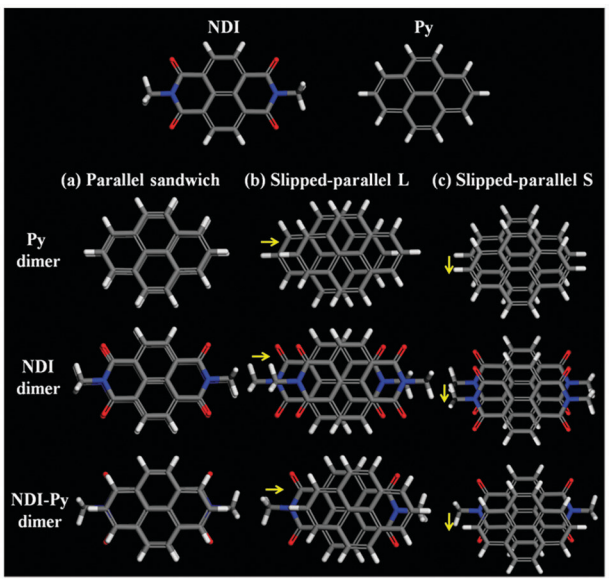

Fig. 1 Parallel dimers of pyrene (Py), naphthalene diimide (NDI) and NDI–Py with configurations of (a) parallel sandwich (S), (b) slipped-parallel L (SP-L), and (c) slipped-parallel S (SP-S).

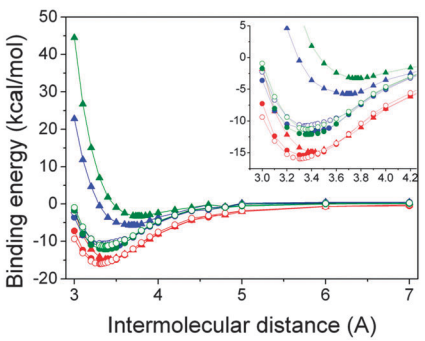

Fig. 2 Binding energy (E) as a function of the distance for S (closed triangles), SP-L (closed circles) and SP-S (open circles) configurations of Py dimer (blue), NDI dimer (green) and NDI–Py dimer (red) calculated at the CP-corrected M06-2X/6-311++G(d,p) level.

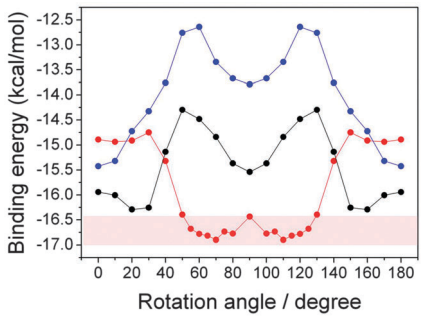

Fig. 3 Binding energies of the NDI–Py dimers as a function of the rotation of Py monomer along its *z* axis. The intermonomer separation is fixed at 3.41 Å for S (red), 3.36 Å for SP-L (blue) and 3.30 Å for SP-S (black). Results are calculated at the CP-corrected M06-2X/6-311++G(d,p) level.

performed using the density functional theory (DFT) with the M06-2X functional and four basis sets of 6-31G(d), 6-31G(d,p), 6-31++G(d,p) and 6-311++G(d,p) were used for comparison. The minimum intermolecular distances and binding energies are given in Table S1 (see the ESI† for details). For the Py dimer, only the 6-311++G(d,p) level of basis set can reproduce the binding energies and interplanar distances (SP-L configuration of Py dimer) when compared to highly extensive DFT-D-BLYP calculations and experimental data.[42–46] Based on the basis set of 6-311++G(d,p), two slipped parallel configurations of SP-L and SP-S are relatively stable than the S geometry by 5.75 and 4.99 kcal mol^{-1}, respectively, probably due to the larger electron exchange repulsion in the S configuration of the Py dimer.[41] Furthermore, the SP-L configuration has a larger binding energy than that of the SP-S by 0.76 kcal mol^{-1}, which indicates that the π–π interactions in the SP-L are stronger than those of the SP-S. It is interesting to note that the displaced structure of the SP-L of Py dimers, that resembles the crystal structure of graphite, has been found to be the most stable isomer.[42–44]

For the NDI dimer, from the binding energies, the dimers of SP-S and SP-L configurations are found to be strongly bound with respect to that of S by 7.99 and 8.80 kcal mol^{-1}, respectively. In addition, the SP-L is slightly stable than the SP-S by 0.81 kcal mol^{-1}. The optimized interplanar distances are nearly identical for two slipped parallel configurations (3.38 Å for SP-L, 3.37 Å for SP-S) whereas the S configuration showed a larger intermolecular distance of 3.77 Å. These results revealed that the electrostatic repulsion between the end-capped diimide moieties in the S configuration is greater than those of SP-L and SP-S. For the NDI–Py dimer, the optimized distances between Py and NDI in the three configurations are close to each other (3.41 Å for S, 3.36 Å for SP-L and 3.30 Å for SP-S). The binding energies for S, SP-L and SP-S configurations are calculated to be −14.98, −15.43 and −15.95 kcal mol^{-1}, respectively. Comparison of the Py, NDI as well as NDI–Py dimers shows that the binding energies are relatively larger in magnitude for the NDI–Py dimer (Fig. 2), and the difference of binding energies and optimized interplanar distances between

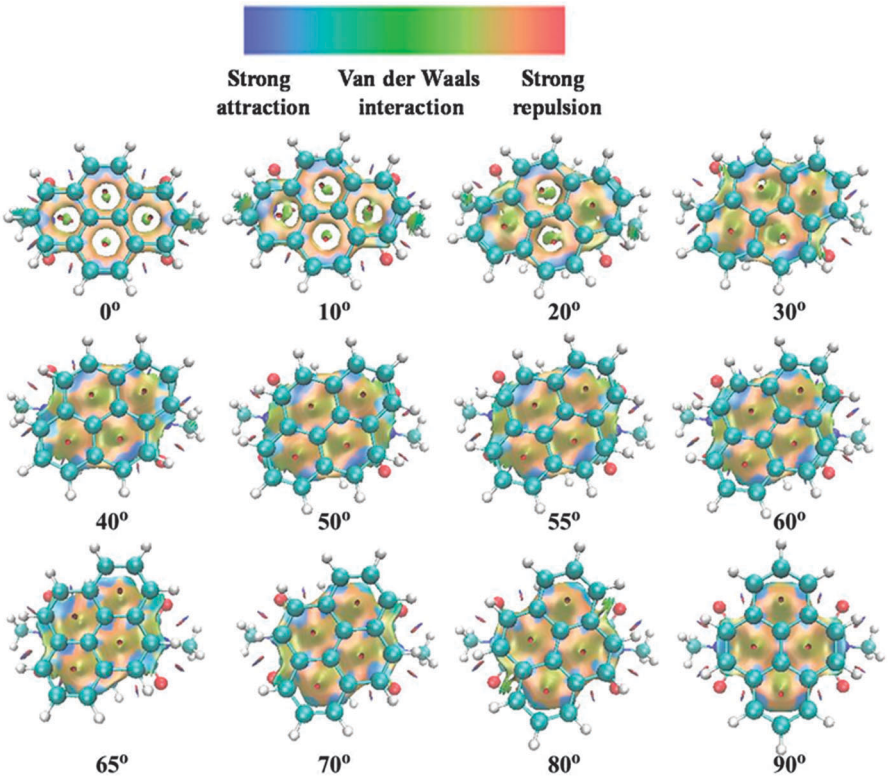

Fig. 4 Visualization of the weak interactions for NDI–Py dimers in the S configuration (top view) in real space. The gradient isosurface method was used and the scale runs from −0.008 (min) to 0.008 (max).

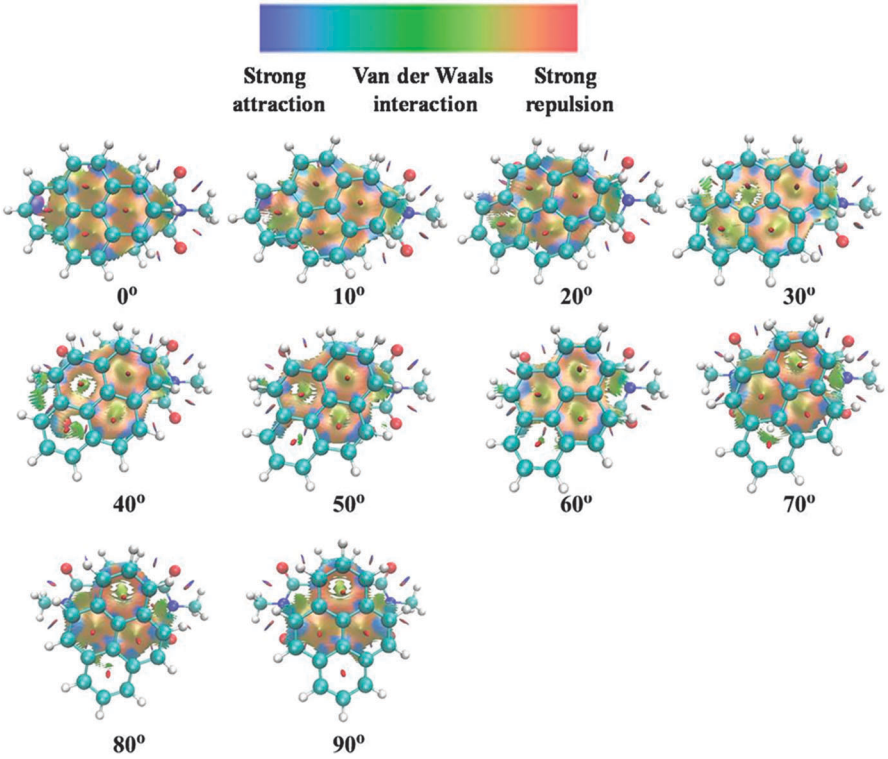

Fig. 5 Visualization of the weak interactions for NDI–Py dimers in the SP-L configuration (top view) in real space. The gradient isosurface method was used and the scale runs from −0.008 (min) to 0.008 (max).

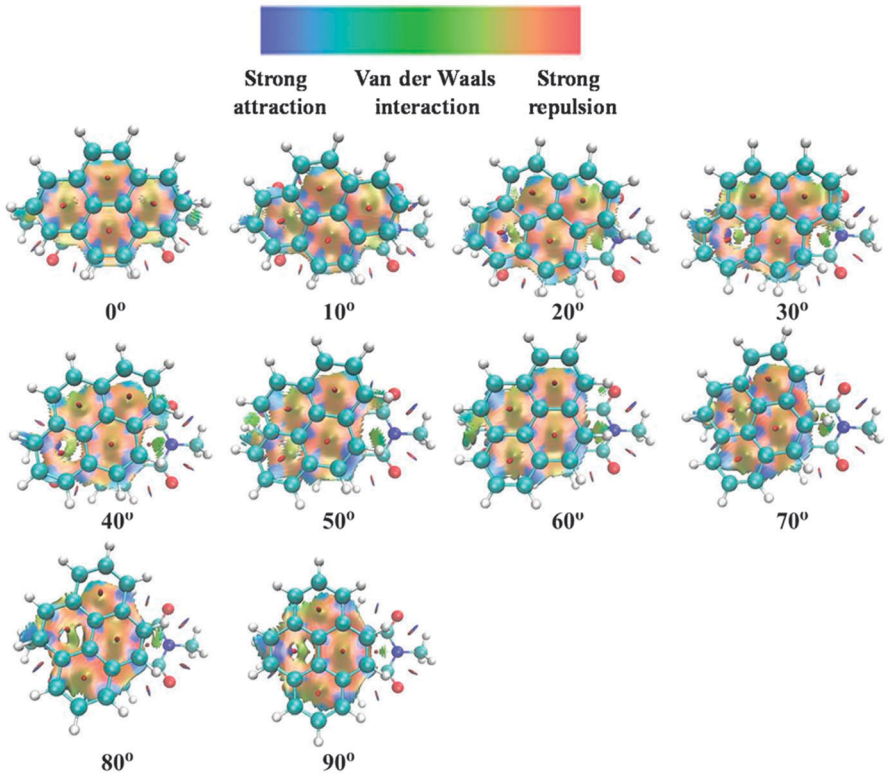

Fig. 6 Visualization of the weak interactions for NDI-Py dimers in the SP-S configuration (top view) in real space. The gradient isosurface method was used and the scale runs from −0.008 (min) to 0.008 (max).

S, SP-L and SP-S configurations of NDI–Py dimers are less than 1 kcal mol^{-1} and 0.1 Å, owing to the electron-rich and electron-deficient nature of the Py and NDI, respectively, which also enhances the stabilization energy of the NDI–Py relative to the NDI and Py dimers.

The X-ray experimental description of the NDI–Py dimer was reported by Wilson *et al.*[28] The interplanar distance of the heterodimer is ~3.4 Å with the rotation of NDI or Py by ~53°. Despite the interactions between $LUMO_{NDI}$ and $HOMO_{Py}$ that can partially explain this phenomenon,[28] the origin of the intermolecular interactions leading to the rotated packing of NDI–Py complexes is still unclear. In order to address this issue, three rotational potential energy curves of S, SP-L and SP-S are depicted in Fig. 3, which quantify the extent to which the intermolecular interaction of the NDI–Py dimer is angular dependent. The NDI monomer is held fixed while the Py monomer rotates along its *z* axis at a fixed separation of 3.41 Å, 3.36 Å and 3.30 Å for S, SP-L and SP-S configurations, respectively. The rotation angles and the corresponding binding energies were calculated at the CP-corrected M06-2X/6-311++G(d,p) level (Fig. 3 and Table S2, ESI†). We found that the face-to-face packing of S configuration is not the minimum energy among these three configurations; a spin angle of approximately 70° is 2.01 kcal mol^{-1} lower in energy compared to that of 0°. Notably, the potential energy curves are very flat for rotation angles larger than 50°. The cofacial (0°) structure of the SP-L is the lowest energy point on the curve, and the SP-S shows that the 20° point is the minimum energy configuration. In comparison to these values, the absolute minimum for S configuration is obtained with a rotation angle ~70°. In consideration of the thermal energy at room temperature,

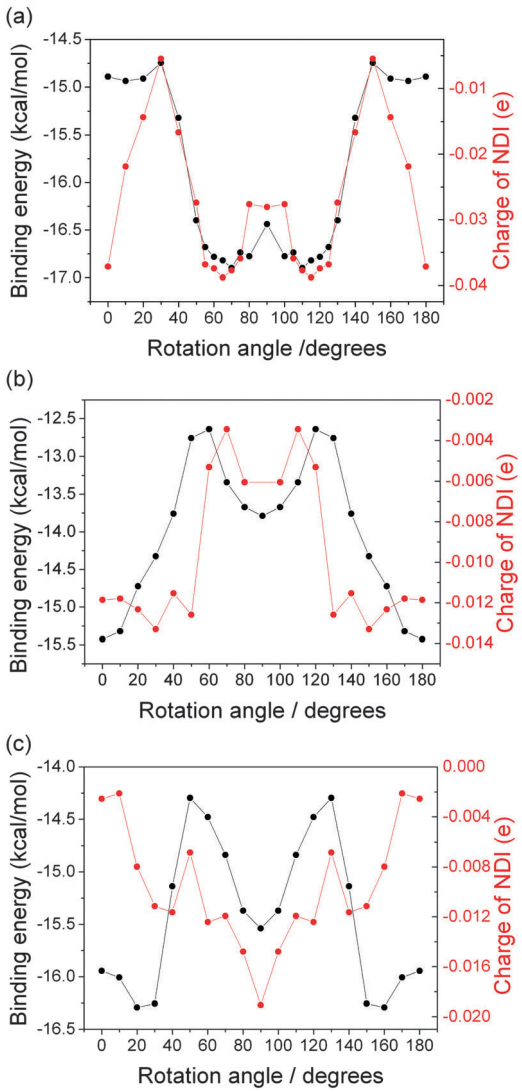

Fig. 7 The potential energy curves of total charges of NDI (closed red circles) as a function of rotation angle of Py monomer along its *z* axis for NDI–Py dimers in the (a) S, (b) SP-L and (c) SP-S configurations. The binding energies as a function of rotation angles of Py monomer (closed black circles) are presented for comparison.

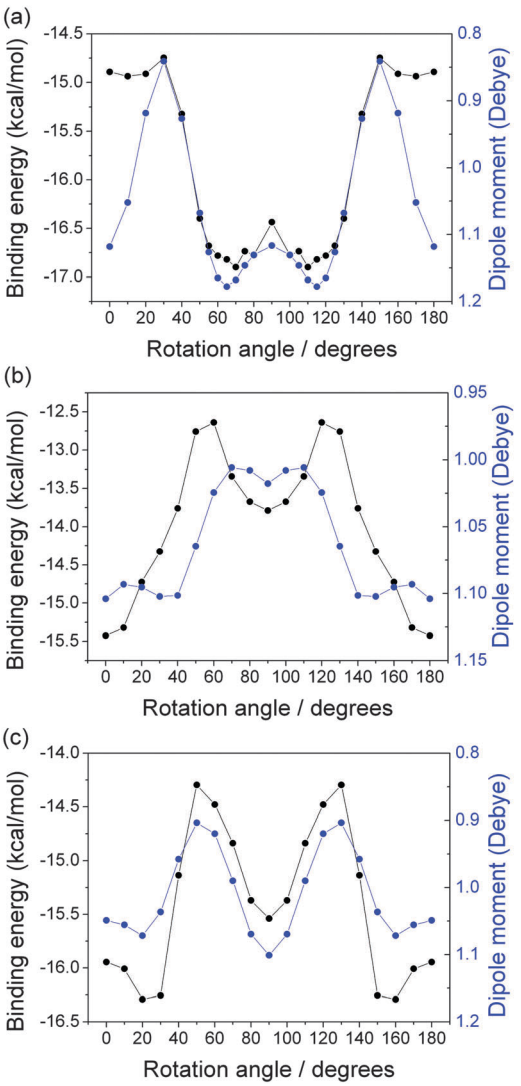

Fig. 8 The potential energy curves of dipole moments (closed blue circles) as a function of rotation angles of Py monomer along its *z* axis for NDI–Py dimers in the (a) S, (b) SP-L and (c) SP-S configurations. The binding energies as a function of rotation angles of Py monomer (closed black circles) are presented for comparison.

the reasonable rotation angles for the complexes will be larger than 50° (pink color in Fig. 3). As mentioned above, the experimental determination of the geometric structure of the NDI–Py molecule leads to the conclusions: Wilson *et al.* have observed, from X-ray diffraction experiments, a rotation angle of about 53° for the NDI–Py packing in the crystal. The experimental result can be reconciled by realizing the potential energy plot in Fig. 3 in which the potential energy curve is shallow for rotation angles larger than 50°. To gather more insight into the packing of the NDI–Py complex, we used the gradient isosurface method of DFT to characterize the non-covalent interactions for rotated NDI–Py dimers. The gradient isosurface method is based on electron density, which is useful to study the signature of non-covalent interactions in real space.[39] The visualization of the π–π interactions in the NDI–Py dimers in real space was done using gradient isosurfaces with a scale running from −0.008 (min) to 0.008 (max). In Fig. 4, the results revealed that the NDI–Py dimers in the S configuration with the rotation angles larger than 50° have a continuous wave function overlap with electronic attraction effect, van der Waals effect and some weak repellent effect. However, the 0° configuration has a discontinuous wave function overlap and almost dominant by the repellent effect. In contrast, the NDI–Py dimers in the SP-L and SP-S configurations with the rotation angles larger than 10–20° have discontinuous wave function overlap and the 0° configurations have continuous wave function overlap (Fig. 5 and 6). These results are consistent with the energy trends, as the potential energy curves shown in Fig. 3.

As D–A assemblies possess attractive optical and electronic properties, including efficient charge separation and transport, understanding of the nature of the intermolecular interactions such as π-stacking and charge-transfer interactions in the NDI–Py dimer system should be potentially useful. Therefore, the natural bond orbital (NBO) analysis was used since it provides an efficient method for studying intra- and/or intermolecular interactions.[47] We calculated the atomic charges of NDI–Py heterodimers as well as NDI and Py monomers for comparison (see Tables S3–S6 in the ESI† for details). Fig. 7 and 8 show the evolution of rotation angles with the total charges on NDI and dipole moments of NDI–Py dimers with the S, SP-L and SP-S configurations. Importantly, for the S configuration, the trend of the total charges and dipole moments are similar to the binding energies when the rotation angle is larger than 30° whereas an inconsistency was found for the rotation angles from 0° to 30°. According to the charge distribution and dipole moment analyses of NDI–Py dimers, both the 0° and ∼70° configurations have significant charge-transfer characters, thus implying that the charge-transfer attractions are not the major contribution to the potential energy curve of binding energies. Notably, for the SP-L and SP-S configurations, the trend of the total charges, dipole moments and the binding energies are similar when the rotation angle is larger than 40°. These results revealed the NDI–Py dimers with rotation angles less than 30° for the S configuration and 40° for the SP-L and SP-S configurations, there is little theoretical evidence for the correlation of binding energies and charger transfer characters.

4. Conclusions

In summary, we have presented a quantum-chemical description for a series of homo- and heterodimers. A series of structural and physical properties have been calculated including geometry, binding energy, dipole moment, population charge distribution, and visualization of the interactions in real space. We found that the relative stable structures of NDI–Py dimers are obtained for parallel sandwich (S) configuration with an intermolecular separation of 3.41 Å and rotation angles larger than 50°, which is consistent with the X-ray experimental data reported by Wilson *et al.*[28] In addition, we found that the trend of the total charges and dipole moments is similar to the binding energies when the rotation angle is larger than 30° whereas an inconsistency was found for the spin angles <30°. Based on the calculations, we recommend using the term charge-transfer interactions in the discussion of non-covalent binding for the rotation of D–A complexes with care. In this work, we provide a representative example of how a detailed analysis of a series of packing structures has been useful in providing deeper insight into the understanding of intermolecular interactions in π-conjugated D–A materials.

Conflicts of interest

The authors declare no competing financial interests.

Acknowledgements

This work has been financially supported by the National Science Council of the Republic of China, Taiwan (Grant No. NSC 102-2113-M-009-006-MY2 and NSC 102-2633-M-009-001-). This work is also supported by the "Aim for the Top University" program of the National Chiao Tung University and Ministry of Education, Taiwan, R.O.C. We are also grateful to the National Center for High-performance Computing of Taiwan for computer time and facilities.

References

1 H. Kar, M. R. Molla and S. Ghosh, *Chem. Commun.*, 2013, **49**, 4220–4222.
2 L. Zang, Y. Che and J. S. Moore, *Acc. Chem. Res.*, 2008, **41**, 1596–1608.
3 Z. Chen, A. Lohr, C. R. Saha-Möllera and F. Würthner, *Chem. Soc. Rev.*, 2009, **38**, 564–584.
4 Y. Tatewaki, T. Hatanaka, R. Tsunashima, T. Nakamura, M. Kimura and H. Shirai, *Chem. – Asian J.*, 2009, **4**, 1474–1479.
5 L. Zhu, Y. Yi, Y. Li, E.-G. Kim, V. Coropceanu and J.-L. Brédas, *J. Am. Chem. Soc.*, 2012, **134**, 2340–2347.
6 R. Bhosale, J. Míšek, N. Sakai and S. Matile, *Chem. Soc. Rev.*, 2010, **39**, 138–149.
7 H. Y. Au-Yeung, G. D. Pantos and J. K. M. Sanders, *Proc. Natl. Acad. Sci. U. S. A.*, 2009, **106**, 10466–10470.
8 P. Talukdar, G. Bollot, J. Mareda, N. Sakai and S. Matile, *J. Am. Chem. Soc.*, 2005, **127**, 6528–6529.

9 W. Pisula, M. Kastler, D. Wasserfallen, J. W. F. Robertson, F. Nolde, C. Kohl and K. Müllen, *Angew. Chem., Int. Ed.*, 2006, **45**, 819–823.
10 V. J. Bradford and B. L. Iverson, *J. Am. Chem. Soc.*, 2008, **130**, 1517–1524.
11 S. De and S. Ramakrishnan, *Macromolecules*, 2009, **42**, 8599–8603.
12 J. Li, L. Guo, L. Zhang, C. Yu, L. Yu, P. Jiang, C. Wei, F. Qin and J. Shi, *Dalton Trans.*, 2009, 823–831.
13 H. Shao, T. Nguyen, N. C. Romano, D. A. Modarelli and J. R. Parquette, *J. Am. Chem. Soc.*, 2009, **131**, 16374–16376.
14 K. V. Rao, K. Jayaramulu, T. K. Maji and S. J. George, *Angew. Chem., Int. Ed.*, 2010, **49**, 4218–4222.
15 J. Zhang, H. Geng, T. S. Virk, Y. Zhao, J. Tan, C.-an. Di, W. Xu, K. Singh, W. Hu, Z. Shuai, Y. Liu and D. Zhu, *Adv. Mater.*, 2012, **24**, 2603–2607.
16 J. J. Tan, Z. Ma, W. Xu, G. Zhao, H. Geng, C. Di, W. Hu, Z. Shuai, K. Singh and D. Zhu, *J. Am. Chem. Soc.*, 2013, **135**, 558–561.
17 A. S. Tayi, A. K. Shveyd, A. C.-H. Sue, J. M. Szarko, B. S. Rolczynski, D. Cao, T. J. Kennedy, A. Sarjeant, C. L. Stern, W. F. Paxton, W. Wu, S. K. Dey, A. C. Fahrenbach, J. R. Guest, H. Mohseni, L. X. Chen, K. L. Wang, J. F. Stoddart and S. I. Stupp, *Nature*, 2012, **488**, 485–489.
18 A. Jain, K. V. Rao, U. Mogera, A. A. Sagade and S. J. George, *Chem. – Eur. J.*, 2011, **17**, 12355–12361.
19 A. A. Sagade, K. V. Rao, U. Mogera, S. J. George, A. Datta and G. U. Kulkarni, *Adv. Mater.*, 2013, **25**, 559–564.
20 L. Schmidt-Mende, A. Fechtenkötter, K. Müllen, E. Moons, R. H. Friend and J. D. MacKenzie, *Science*, 2001, **293**, 1119–1122.
21 V. Percec, M. Glodde, T. K. Bera, Y. Miura, I. Shiyanovskaya, K. D. Singer, V. S. K. Balagurusamy, P. A. Helney, I. Schnell, A. Rapp, H. W. Spiess, S. D. Hudson and H. Duan, *Nature*, 2002, **417**, 384–387.
22 N. Sakai, J. Mareda, E. Vauthey and S. Matile, *Chem. Commun.*, 2010, **46**, 4225–4237.
23 B. J. H. Oh, S. L. Suraru, W. Y. Lee, M. Könemann, H. W. Höffken, C. Röger, R. Schmidt, Y. Chung, W. C. Chen, F. Würthner and Z. Bao, *Adv. Funct. Mater.*, 2010, **20**, 2148–2156.
24 M. R. Molla and S. Ghosh, *Chem. – Eur. J.*, 2012, **18**, 9860–9869.
25 A. Das and S. Ghosh, *Angew. Chem., Int. Ed.*, 2014, **53**, 1092–1097.
26 K. Jalani, M. Kumar and S. J. George, *Chem. Commun.*, 2013, **49**, 5174–5176.
27 Y. Kim, J. Hong, J. H. Oh and C. Yang, *Chem. Mater.*, 2013, **25**, 3251–3259.
28 M. D. Gujrati, N. S. S. Kumar, A. S. Brown, B. Captain and J. N. Wilson, *Langmuir*, 2011, **27**, 6554–6558.
29 N. S. S. Kumar, M. D. Gujrati and J. N. Wilson, *Chem. Commun.*, 2010, **46**, 5464–5466.
30 Y. Zhao and D. G. Truhlar, *Theor. Chem. Acc.*, 2008, **120**, 215–241.
31 E. G. Hohenstein, S. T. Chill and C. D. J. Sherrill, *J. Chem. Theory Comput.*, 2008, **4**, 1996–2000.
32 R. Podeszwa and K. Szalewicz, *Phys. Chem. Chem. Phys.*, 2008, **10**, 2735–2746.
33 J. Vura-Weis, M. A. Ratner and M. R. Wasielewski, *J. Am. Chem. Soc.*, 2010, **132**, 1738–1739.
34 M. J. Frisch, G. W. Trucks, H. B. Schlegel, G. E. Scuseria, M. A. Robb, J. R. Cheeseman, G. Scalmani, V. Barone, B. Mennucci, G. A. Petersson, H. Nakatsuji, M. Caricato, X. Li, H. P. Hratchian, A. F. Izmaylov, J. Bloino, G. Zheng, J. L. Sonnenberg, M. Hada, M. Ehara, K. Toyota, R. Fukuda, J. Hasegawa, M. Ishida, T. Nakajima, Y. Honda, O. Kitao, H. Nakai, T. Vreven, J. A. Montgomery, Jr., J. E. Peralta, F. Ogliaro, M. Bearpark, J. J. Heyd, E. Brothers, K. N. Kudin, V. N. Staroverov, T. Keith, R. Kobayashi, J. Normand, K. Raghavachari, A. Rendell, J. C. Burant, S. S. Iyengar, J. Tomasi, M. Cossi, N. Rega, J. M. Millam, M. Klene, J. E. Knox, J. B. Cross, V. Bakken, C. Adamo, J. Jaramillo, R. Gomperts, R. E. Stratmann, O. Yazyev, A. J. Austin, R. Cammi, C. Pomelli, J. W. Ochterski, R. L. Martin, K. Morokuma, V. G. Zakrzewski, G. A. Voth, P. Salvador, J. J. Dannenberg, S. Dapprich, A. D. Daniels, O. Farkas, J. B. Foresman, J. V. Ortiz, J. Cioslowski and D. J. Fox, *Gaussian 09 (Revision B.01)*, Gaussian, Inc., Wallingford, CT, 2010.
35 S. F. Boys and F. Bernardi, *Mol. Phys.*, 1970, **19**, 553–566.
36 A. E. Reed, L. A. Curtiss and F. Weinhold, *Chem. Rev.*, 1988, **88**, 899–926.
37 E. D. Glendening, A. E. Reed, J. E. Carpenter and F. Weinhold, *J. Am. Chem. Soc.*, 1998, **120**, 12051–12068.
38 T. Lu and F. Chen, *J. Comput. Chem.*, 2012, **33**, 580–592.
39 E. R. Johnson, S. Keinan, P. Mori-Sánchez, J. Contreras-García, A. J. Cohen and W. Yang, *J. Am. Chem. Soc.*, 2010, **132**, 6498–6506.
40 J. Contreras-García, E. R. Johnson, S. Keinan, R. Chaudret, J.-P. Piquemal, D. N. Beratan and W. Yang, *J. Chem. Theory Comput.*, 2011, **7**, 625–632.
41 S. M. Ryno, C. Risko and J.-L. Brédas, *J. Am. Chem. Soc.*, 2014, **136**, 6421–6427.
42 C. Gonzalez and E. C. Lim, *J. Phys. Chem. A*, 2003, **107**, 10105–10110.
43 S. Grimme, *J. Comput. Chem.*, 2004, **25**, 1463–1473.
44 J. Li, Y. Liu, Y. Qian, L. Li, L. Xie, J. Shang, T. Yu, M. Yi and W. Huang, *Phys. Chem. Chem. Phys.*, 2013, **15**, 12694–12701.
45 M. P. Waller, H. Kruse, C. Muck-Lichtenfeld and S. Grimme, *Chem. Soc. Rev.*, 2012, **41**, 3119–3128.
46 R. Peverati and K. K. Baldridge, *J. Chem. Theory Comput.*, 2008, **4**, 2030–2048.
47 M. Snehalatha, C. Ravikumar, I. Hubert Joe, N. Sekar and V. S. Jayakumar, *Spectrochim. Acta*, 2009, **72**, 654–662.

